

Convolutional Neural Networks combined with Runge-Kutta Methods

Mai Zhu

Northeastern University China

zhumai@stumail.neu.edu.cn

Chong Fu

Northeastern University China

fuchong@mail.neu.edu.cn

Abstract

A convolutional neural network for image classification can be constructed following some mathematical ways since it models the ventral stream in visual cortex which is regarded as a multi-period dynamical system. In this paper, a new point of view is proposed for constructing network models as well as providing a direction to get inspiration or explanation for neural network. If each period in ventral stream was deemed to be a dynamical system with time as the independent variable, there should be a set of ordinary differential equations (ODEs) for this system. Runge-Kutta methods are common means to solve ODE. Thus, network model ought to be built using these methods. Moreover, convolutional networks could be employed to emulate the increments within every time-step. The model constructed in the above way is named Runge-Kutta Convolutional Neural Network (RKNet). According to this idea, Dense Convolutional Networks (DenseNets) and Residual Networks (ResNets) were varied to RKNet. To prove the feasibility of RKNet, these variants were verified on benchmark datasets, CIFAR and ImageNet. The experimental results show that the RKNet transformed from DenseNets gained similar or even higher parameter efficiency. The success of the experiments denotes that Runge-Kutta methods can be utilized to construct convolutional neural networks for image classification efficiently. Furthermore, the network models might be structured more rationally in the future basing on RKNet and priori knowledge.

1. Introduction

All this time, many investigations were devoted to search the relations between artificial neural networks and the visual system of brain in order to gain inspiration to construct new network models. Inspired by neuroscience, a recurrent convolutional neural network (RCNN) was proposed for object recognition because recurrent connections are abundant in the visual system of brain [10]. However, ResNets which are feed-forward network models have retrieved a great success on several popular vision bench-

marks in 2015 [5]. After that, the architecture of ResNets was researched combining with Recurrent Neural Network (RNN) for trying to know the relations between residual learning and visual cortex. As a result, the multi-state time-invariant recurrent networks that reflected the multi-stage processing in the primate visual cortex were found performing as well as very deep residual networks without shared weights [11]. Therefore, recurrent architecture should be paid attention to while modeling image classification. In addition, DenseNets which are state-of-the-art models more recently have the similar multi-period structure though they have no recurrence [7]. Thus, a multi-period recurrent network model, i.e. a biologically-plausible model of the ventral stream in visual cortex, might be an appropriate model for image classification.

On the other hand, only combining convolutional neural network (CNN) with neuroscience is not adequate. Mathematical approaches should be equally valid in the area of designing network topology. Since the ventral stream in visual cortex is deemed to be a multi-period dynamical system with time as the independent variable [11], there should be a series of ODEs to describe this system. Runge-Kutta methods are widely-used means to solve ODE in numerical analysis. Moreover, they are iterative methods so they can present recurrences. Consequently, these methods could be used to try building network models for visual processing. Furthermore, the mathematical structure of visual system might be disclosed along this way.

It is not the first time for using Runge-Kutta methods to construct neural network. Runge-Kutta Neural Network (RKNN) has been proposed for identification of unknown dynamical systems which was time-invariant [17]. Yet it has not been used for modeling visual processing till now and has no convolution either. In order to try applying Runge-Kutta methods to image classification, preconditions are assumed in this paper as following. Firstly, the image classification procedures were multi-period. Secondly, each period in classification process was presumed as a dynamical system with time as the independent variable. Thirdly, there was no connection between non-adjacent periods. In terms of these preconditions, a sort of network model named

RKNet is proposed in this paper.

In a RKNet, a period of the network is constructed by a s -stage Runge-Kutta method taking r time-steps. Nevertheless, Runge-Kutta methods need specific ODEs to accomplish calculation of increments in each time-step. There is, of course, no any explicit equation to represent the visual processing up to now whereas CNN could learn to approximate them. On the contrary, these ODEs might be revealed after CNN imitated them precisely. The specific equations for image classification are not included in this paper. There is a long way to go for making them clear but the proposed novel standpoint of view should be a good beginning.

In the field of image classification, CNN used to be utilized for emulating the state trajectory before classifier directly. Consequently, there is an issue when CNN simulates increments in each time-step of a RKNet. That is the complexity of these convolutional subnets. To be specific, the network model would be more complicated as a whole if these subnets are too complex. This issue determines whether Runge-Kutta methods are suitable to be adopted to construct neural network for visual processing in practice. Moreover, it can only be clarified by experiments since there is no explicit equation. By observing the architecture of DenseNets and ResNets, it was discovered that they could be transformed to RKNet easily. Thus, they fit to be experimental objects for verifying the feasibility of RKNet. If a RKNet variant could achieve the comparable accuracy with similar parameters to the original model, the conclusion should be drawn that Runge-Kutta methods were able to be employed to model image classification efficiently.

To evidence the above deduction, some DenseNets and ResNets are varied and then evaluated on benchmark datasets, CIFAR-10, CIFAR-100 [8] and ILSVRC2012 classification dataset [14]. Experimental results in this paper show that some variants are superior to the original models on parameter efficiency. Hence, Runge-Kutta methods are appropriate for modeling the process of image classification.

The rest of the paper is organized as follows. The related work is reviewed in Section 2. Then, the architecture of RKNet and the transformation approaches for varying DenseNets and ResNets to RKNet are described in Section 3. After that, the performance of the variants of DenseNets and ResNets is evaluated in Section 4. At the end, the conclusion is drawn in Section 5.

2. Related Work

ResNets have gained much attention over the past few years since they had obtained impressive achievements on many challenging image tasks, such as ImageNet [14] and COCO object detection [12]. ResNets are very deep feed-forward networks with the shortcuts for identity mappings. This kind of structure is regarded as an unfolded shallow

RNN which implements a discrete dynamical system by the paper [11]. This dynamical system represents the processing through the ventral stream of the primate visual cortex. The ventral stream is associated with visual perception and passes several visual areas, i.e. V1, V2, V4, IT [2]. Each visual area is considered as a processing period. Furthermore, it has been shown that recurrent connections existed richly in the neocortex by anatomical evidences [1]. These recurrent connections within each visual area are modeled as a recurrent network in [11]. Some biologically-plausible multi-state recurrent networks corresponding to the multi-stage processing in the ventral stream have been evaluated on CIFAR-10 in that research. What needs to be noted is that *state* and *stage* in their descriptions both denote period but not the state of dynamical system and the stage of Runge-Kutta methods respectively. According to their experiments, the multi-state recurrent network model not sharing weights has higher accuracy than the one that shared weights across time within every period. However, they both obtain lower error rates with narrowed gap between them after the number of periods increases. In addition, 3-state fully RNN gains the comparable validation error with ResNets whereas 3-state adjacently RNN gets only a little higher error rate than it with much fewer parameters. Thereinto, *fully* denotes that every period has transition to any period including itself while *adjacently* means that each period has transitions to adjacent periods and itself. From that study, it can be drawn that emulating image classification as a 3-state adjacently RNN with shared weights across time within each period is able to achieve competitive performance on CIFAR-10.

DenseNets are the state-of-the-art network models beyond ResNets later. The dense connectivity in them is the main difference from the previous network models. It means the direct connections from any layer to all subsequent layers. The dense blocks of DenseNets can be deemed to correspond to the visual areas in ventral stream. Hence, DenseNets are multi-period CNNs. Specifically, DenseNets for ImageNet are 4-period CNNs while the ones for CIFAR are 3-period CNNs.

Now that a visual area is thought of as a dynamical system with time as the independent variable no matter whether it is time-invariant or not, there should be a set of ODEs to describe this system. Consequently, some mathematical approaches for handling those ODEs might be employed to construct the network model. Runge-Kutta methods are commonly utilized to solve ODE in numerical analysis. Moreover, these methods are iterative. The iterations of time-steps in the periods seem like the recurrent connections within visual areas. Furthermore, they have been lent to construct neural network, which was known as RKNN, for identification of unknown dynamical systems described by ODEs in high accuracy. In [17], the neural

network that directly learns the state trajectory of a dynamical system is called a direct-mapping neural network (DMNN) while the one which learns the changing rates of system states is named a RKNN. Hence, AlexNet [9], VGGNet [15], GoogLeNet [16], ResNet and so on can also be called DMNNs. RKNN was proposed to eliminate several drawbacks of DMNNs such as not easy obtaining high accuracy for the multistep prediction of state trajectories. The paper [17] shows quantitatively that the RKNN has higher prediction accuracy and better generalization capability than the conventional DMNN in theory. At the same time, it provides two experiments to support the theoretical results too. Therefore, it is reasonable to believe that Runge-Kutta methods can be adopted in network architecture for image classification. Additionally, the emulation of image classification might benefit from these methods when the convolutional subnet simulated the changing rates of the dynamical system states as precisely as possible.

3. RKNets

There are three portions in RKNets at macro level. They are preprocessor, multi-periods and postprocessor in turn. The preprocessor processes the raw image and then inputs the result to the first period. It mainly emulates the process that visual information coming from the eye reaches the visual cortex. The postprocessor deals with the output from the last period and then inputs the result to the classifier to make a decision. The periods between the above two portions are split by transition layers. These periods imitate the dynamical systems with time as the independent variable which are assumed to represent visual areas in the ventral stream of visual cortex. Temporal discretization is introduced to predict state trajectory. In other words, each period of RKNet is split into time-steps as shown in Figure 1. A variety of Runge-Kutta methods taking various time-steps can be adopted in the imitation. The network models name after these methods, such as RKNet-3×2.4×1.2×5.1×1. To be specific, the suffix in the name of a RKNet is composed of several $s \times r$ parts, each of which stands for the numerical analysis method in corresponding period by turns. Thereinto, s denotes the stage of Runge-Kutta method while r is the number of time-steps. The amount of these parts equals the number of periods. s or r can be various in different periods. This nomenclature will be used throughout this paper.

A dynamical system with time as the independent variable for a period is supposed to be described by the following ODE:

$$\frac{dy}{dt} = f(t, y), \quad y(t_0) = y_0. \quad (1)$$

where y is a vector, the dimension of which equals the dimension of the dynamical system. Nevertheless, dimen-

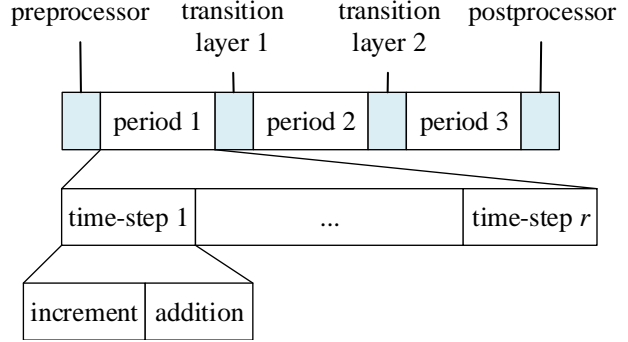


Figure 1. Architecture of a 3-period RKNet. r is the total number of time-steps. To emulate ODE is the key point to get increment.

sionality reduction is always carried out in emulation when the real dimension is too high. Eq. (1) represents the changing rates of system states. Any changing rate is a function of time and all the system states.

The family of explicit Runge-Kutta methods is given by the following equations:

$$y_{n+1} = y_n + h \sum_{i=1}^s b_i k_i, \quad t_{n+1} = t_n + h \quad (2)$$

where

$$\begin{aligned} k_1 &= f(t_n, y_n), \\ k_2 &= f(t_n + c_2 h, y_n + h(a_{21} k_1)), \\ k_3 &= f(t_n + c_3 h, y_n + h(a_{31} k_1 + a_{32} k_2)), \\ &\dots \\ k_i &= f\left(t_n + c_i h, y_n + h \sum_{j=1}^{i-1} a_{ij} k_j\right). \end{aligned} \quad (3)$$

Thereinto, h is time-step size. In Eq. (2), the integer s is the stage of Runge-Kutta methods. Eq. (2) approximates the solution to Eq. (1) at time t_{n+1} , i.e. $y(t_{n+1})$. y_n is the approximation of $y(t_n)$ except y_0 that is the given initial value. Eq. (3) is the general term formula. All the coefficients in Eq. (2) and (3) except h need to be provided for an adopted particular Runge-Kutta method in common numerical analysis.

From these equations of explicit Runge-Kutta methods, it denotes clearly that each k_i is a function of time, y_n and all the elements from k_1 to k_{i-1} . Furthermore, y_{n+1} is a linear function of y_n and all the elements from k_1 to k_s . As an observation basing on these equations, every dense block together with part of the following computation in DenseNets can be regarded as a period adopting a s -stage Runge-Kutta method taking only one time-step approximatively. In a dense block, the i th group of extra feature-maps gained

by growing m times successively corresponds to $hb_i k_i$ in Eq. (2) when the number of the inputted feature-maps is m times of growth rate where m is an integer. Hence, the times of growth divided by m is the total number of k_i , i.e. s . The transition layers and the postprocessor can be considered to contain the linear operation of Eq. (2) implicitly in their convolutions of y_n and all the elements from $hb_1 k_1$ to $hb_s k_s$. In addition, $hb_i k_i$ can be described by the equation below according to Eq. (3).

$$\begin{aligned} hb_i k_i &= hb_i f \left(t_n + c_i h, y_n + h \sum_{j=1}^{i-1} a_{ij} k_j \right) \quad (4) \\ &= F_i(t_n, h, y_n, k_1, \dots, k_{i-1}). \end{aligned}$$

Therefore, every subnet for a group of growth in DenseNets can be thought of to simulate the function $F_i(\cdot)$ integrally without definite coefficients and even without explicit time input. These aspects affect the accuracy of simulation. They need further investigation. Since the main purpose of this paper is to utilize Runge-Kutta methods to simulate each period, the emphasis is put on the verification of feasibility. Therefore, these issues are not studied temporarily but accepted or avoided so long as RKNets could be as parameter efficient as DenseNets or even surpass them. As a result, all the coefficients in Eq. (4) will be learned by training in feasibility verification for the convenience of comparison. In addition, a further hypothesis is made to eliminate the influence of time in order to simplify the verification. It is that the right-hand side of Eq. (1) did not explicitly depend on the time variable or the time variable had so few effects on Eq. (1) that it could be ignored in the emulation. In other words, each period is supposed to be a time-invariant system or an approximate one. On the basis of this assumption, time variable is unnecessary to be inputted explicitly any more.

A time-invariant system for a period is described by the following ODE:

$$\frac{dy}{dt} = g(y), \quad y(t_0) = y_0. \quad (5)$$

Eq. (3) can be adapted for time-invariant system as below:

$$k_i = g \left(y_n + h \sum_{j=1}^{i-1} a_{ij} k_j \right). \quad (6)$$

Eq. (4) can be rewritten for time-invariant system as follows:

$$\begin{aligned} hb_i k_i &= hb_i g \left(y_n + h \sum_{j=1}^{i-1} a_{ij} k_j \right) \quad (7) \\ &= G_i(h, y_n, k_1, \dots, k_{i-1}). \end{aligned}$$

Basing on the above hypothesis, RKNet has the advantage in the aspect of parameter efficiency. The weights and biases of different time-steps in a period can be shared with each other for parameter reduction. Moreover, when a multi-stage Runge-Kutta method is adopted, if y_n and all the elements from k_1 to k_{i-1} is inputted to $g(\cdot)$ as a linear combination but not to $G_i(\cdot)$ separately, the weights and biases of the imitation of Eq. (5) can be shared across different stages as well as time-steps. This will reduce the number of parameters further.

Besides, Euler method is one of Runge-Kutta methods. The solution to Eq. (5) at time t_{n+1} is approximated by the equation below using Euler method.

$$y_{n+1} = y_n + hg(y_n), \quad t_{n+1} = t_n + h. \quad (8)$$

A building block in ResNets is similar to Eq. (8). However, there is a ReLU after the addition in every building block. This detail decides that ResNets are not RKNs but DMNNs since a building block learns the state trajectory but not the changing rates of system states. If moving this ReLU to the end of residual mapping, a ResNet will be changed to a RKNet which uses Euler method taking several time-steps in each period. Nevertheless, the variants might not be superior to the original ResNets since the transformation for them is not as reasonable as the rectification for DenseNets. In particular, $hb_i k_i$ should be real number but it cannot be negative due to ReLU as activation function. However, if they could obtain acceptable accuracies in experiments, these variants could also be looked as some efficient instances for RKNet in practice.

Additionally, there are three periods in some DenseNets and ResNets while there are four visual areas in the ventral stream. They could be thought of to fuse the four dynamical systems into three periods.

For the purpose of the feasibility verification for applying RKNet on image classification, DenseNets and ResNets are transformed as follows.

3.1. Transform DenseNets

In macro level, DenseNets are very close to RKNets which adopt multi-stage Runge-Kutta methods taking one time-step in each period. However, there is no clear boundary after periods and before transition layers or postprocessor in DenseNets. To be specific, there is no explicit summation layer for Eq. (2). Therefore, it is essential to add a summation layer at the end of each time-step. As a result, the final output dimension of a dense block is reduced to the input dimension of this block. It will affect the input dimension of the following layers. Nevertheless, for the convenience of comparison, although the input dimensions of the transition layers are reduced, their output dimensions are tried to keep the approximate values to the corresponding original DenseNets in order to maintain the

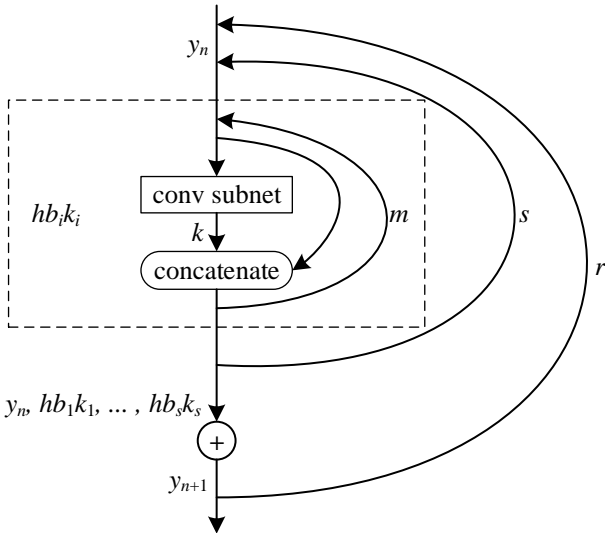


Figure 2. Architecture of a period in RKNet adopting a s -stage Runge-Kutta method taking r time-steps. The convolutional subnet concatenates m times at a growth rate k to generate each $hb_i k_i$ by turns. Thereinto, h is time-step size. b_i is coefficient of some indicated Runge-Kutta method. k_i is the slope of each stage in a time-step. y_n is the approximation of $y(t_n)$ except y_0 that is the given initial value. The portion within dotted line concatenating s times forms a dense block in DenseNet. An explicit summation layer is added after a dense block to complete a time-step. The time-step iterates r times to compose a period.

input dimensions of periods after them. The calculation of these dimensions will follow the subsequent procedures. At first, the number of convolution filters in transition layers of the original DenseNet is divided by growth rate k and then rounded down to an integer m . Secondly, the result is multiplied by the growth rate again to gain a multiple of growth rate as the number of feature-maps inputted to the later dense block, i.e. mk .

What's more, the total rounds of feature-maps growth in a dense block divided by the corresponding m of this block is usually a decimal in original DenseNets. In other words, the integral stage s cannot be obtained for most models in [7]. In this case, the computed results will be round up to integers as the stages for them.

On the basis of the one time-step variants, the stages of Runge-Kutta methods and the numbers of time-steps can be changed to construct more variants with same input dimensions of periods. The growth rate k and each m in every period are responsible for the different dimensions. The recurrent structure for a period basing on DenseNet is shown in Figure 2.

3.2. Transform ResNets

At first, the periods and transition layers in ResNets need be separated from each other because there is no definite divide in the original models. The building blocks in which the input dimension equals to the output dimension are assumed as period blocks whereas the ones in which the output dimension differs from the input dimension are supposed to be transition layers or part of the preprocessor. There are ResNets without bottleneck and the ones with bottleneck. As a result, the specific division of components has a little difference because of the dimensions in the original models.

Moreover, ReLU after the addition in every period block is moved to the end of the residual mapping as a way to simulate $G_i(\cdot)$ in Eq. (7). ReLUs in building blocks of other parts are remained unchanged.

4. Experiments

For the purpose of verifying the feasibility of applying RKNet on image classification, experiments need to be conducted to find out the variants of DenseNets or ResNets which have comparable or even higher accuracies with similar number of parameters to the original network models.

In experiments, the convolution, batch normalization, activation function and pooling layers in variants totally follow the original network models for the convenience of comparison. In addition, there are three periods in some DenseNets and ResNets while some have four periods. Both the three-period variants and the four-period ones are appraised in experiments. What's more, the variants with different stages or time-steps are also assessed as required.

The variants are evaluated on CIFAR-10, CIFAR-100 or ImageNet as needed. The CIFAR-10 dataset is constitutive of 60000 32×32 color images in 10 classes with 5000 training images and 1000 test images per class. The CIFAR-100 is similar to the CIFAR-10 while it has 100 classes containing 500 training images and 100 testing images per class. ImageNet, which indicates ILSVRC2012 classification dataset here, consists of 1.28 million training images and 50000 validation images.

To make sure that the comparisons between the variants and original network models are fair, the Torch implementation of ResNet offered by [3]¹ and the memory efficient implementation of DenseNet basing on the former provided by [13]² are adopted. Only the network models are varied while all the experiment settings remain the same as what were used for DenseNets. The details are as following.

The weights are initialized as in [4]. A weight decay of 0.0001 and a momentum of 0.9 are used. The learning rate is set to 0.1 initially.

¹<https://github.com/facebook/fb.resnet.torch>

²<https://github.com/liuzhuang13/DenseNet/tree/master/models>

| Original model | Depth | Param (M) | Error (%) | Variant | $m1$ (k) | $m2$ (k) | Param (M) | Error (%) | Param with share (M) | Error with share (%) |
|--------------------------|-------|--------------|--------------|--|-----------------|-----------------|--------------|--------------|-------------------------------|-------------------------------|
| DenseNet ($k = 12$) | 40 | 1.0 | 5.24 | RKNet- $6 \times 1_1 \times 1_1 \times 1$ RKNet- $1 \times 6_1 \times 1_1 \times 1$ RKNet- $3 \times 2_1 \times 1_1 \times 1$ | 14 | 26 | 1.85 | 5.00 | - | - |
| DenseNet ($k = 12$) | 100 | 7.0 | 4.10 | RKNet- $16 \times 1_1 \times 1_1 \times 1$ RKNet- $1 \times 16_1 \times 1_1 \times 1$ | 34 | 66 | 11.7 | 4.33 | - | - |
| DenseNet ($k = 24$) | 100 | 27.8 | 3.74 | RKNet- $16 \times 1_1 \times 1_1 \times 1$ RKNet- $1 \times 16_1 \times 1_1 \times 1$ | 34 | 66 | 46.9 | - | - | - |
| DenseNet-BC ($k = 12$) | 100 | 0.75 | 4.51 | RKNet- $8 \times 1_2 \times 1_2 \times 1$ RKNet- $1 \times 8_1 \times 2_1 \times 2$ RKNet- $2 \times 4_2 \times 1_2 \times 1$ | 9 | 12 | 0.91 | 4.67 | - | - |
| DenseNet-BC ($k = 24$) | 250 | 15.1 | 3.62 | RKNet- $21 \times 1_2 \times 1_2 \times 1$ RKNet-$1 \times 21_1 \times 2_1 \times 2$ RKNet- $3 \times 7_2 \times 1_1 \times 2$ | 21 | 31 | 18.4 | 3.57 | - | - |
| DenseNet-BC ($k = 40$) | 190 | 25.4 | 3.46 | RKNet- $16 \times 1_2 \times 1_2 \times 1$ RKNet- $1 \times 16_1 \times 2_1 \times 2$ RKNet- $4 \times 4_2 \times 1_1 \times 2$ | 16 | 23 | 30.4 | - | - | - |
| DenseNet-BC ($k = 24$) | 292 | 20.1 | - | RKNet-$1 \times 24_1 \times 2_1 \times 2$ | 25 | 36 | 17.5 | - | 8.4 | 3.56 |

Table 1. Test errors evaluated on CIFAR-10 with data augmentation. k is growth rate. $m1$ and $m2$ are the number of convolution filters in transition layer 1 and 2 respectively with growth rate k as a unit. $m0$ is always 2. All the RKNets are the variants of corresponding DenseNets in the same row with similar input dimensions of periods. RKNets that outperform DenseNets with fewer parameters and higher accuracies are **bold**.

| Original model | Depth | Param (M) | Error (%) | Variant | $m1$ (k) | $m2$ (k) | Param (M) | Error (%) | Param with share (M) | Error with share (%) |
|--------------------------|-------|--------------|--------------|--|-----------------|-----------------|--------------|--------------|-------------------------------|-------------------------------|
| DenseNet-BC ($k = 12$) | 100 | 0.8 | 22.27 | RKNet- $1 \times 8_1 \times 2_1 \times 2$ | 9 | 12 | 0.7 | 23.10 | 0.3 | 25.33 |
| DenseNet-BC ($k = 24$) | 250 | 15.2 | 17.60 | RKNet- $1 \times 21_1 \times 2_1 \times 2$ | 21 | 31 | 13.3 | 18.90 | 6.4 | 19.65 |
| DenseNet-BC ($k = 40$) | 190 | 25.6 | 17.18 | RKNet- $1 \times 16_1 \times 2_1 \times 2$ | 16 | 23 | 22.4 | 17.95 | 10.5 | 18.86 |
| DenseNet-BC ($k = 24$) | 292 | 20.3 | - | RKNet- $1 \times 24_1 \times 2_1 \times 2$ | 25 | 36 | 17.6 | 18.40 | 8.5 | 19.15 |

Table 2. Test errors evaluated on CIFAR-100 with data augmentation. k is growth rate. $m1$ and $m2$ are the number of convolution filters in transition layer 1 and 2 respectively with growth rate k as a unit. All the RKNets are the variants of corresponding DenseNets in the same row with similar input dimensions of periods.

On CIFAR-10 and CIFAR-100, the models are trained using stochastic gradient descent with a mini-batch size of 64 and a standard data augmentation scheme adopted in [5]. The trainings all run for 300 epochs in which the learning rate is divided by 10 at epoch 150 and 225.

On ImageNet, some models are trained with a batch size of 256 for 90 epochs while the others are trained with a batch size of 128 for 100 epochs because of GPU memory constraints. The specific cases are commented on the experimental data. Scale and aspect ratio augmentation from [16], the standard color augmentation in [9] as well as the photometric distortions from [6] are adopted. The learning rate is lowered by 10 times every 30 epochs. Weight

decay is applied to all weights and biases.

Besides, only the weights and biases of convolutions are shared across time-steps in every period but batch normalizations are not shared for the variants which are marked with share. The specific experimental results are expounded in the chapters below.

4.1. Variants of DenseNets

DenseNets are similar to some RKNets. Every period of a DenseNet is considered to use multi-stage Runge-Kutta method taking only one time-step approximatively. Their variants which use Runge-Kutta methods with various stages taking diverse time-steps in periods according to

| Original model | Param (M) | Top1 (%) | Top5 (%) | Variant | m_3 (k) | Param (M) | Top1 (%) | Top5 (%) | Param (M) | Top1 (%) | Top5 (%) |
|---------------------------|-----------|----------|----------|---|-----------|-----------|----------|----------|-----------|----------|----------|
| DenseNet-121 ($k = 32$) | 7.9 | 25.02 | 7.71 | RKNet-3 \times 1_3 \times 1_3 \times 1_1 \times 1 | 16 | 6.9 | 25.47 | 7.81 | - | - | - |
| | | | | RKNet-1 \times 3_1 \times 3_1 \times 3_1 \times 1 | | 5.8 | 26.24 | 8.38 | 3.8 | 28.51 | 9.72 |
| DenseNet-169 ($k = 32$) | 14.0 | 23.80 | 6.85 | RKNet-1 \times 3_1 \times 3_1 \times 4_1 \times 2 | 20 | 10.8 | 25.22 | 7.74 | 5.0 | 27.49 | 8.94 |
| DenseNet-201 ($k = 32$) | 19.8 | 22.58 | 6.34 | RKNet-1 \times 3_1 \times 3_1 \times 6_1 \times 2 | 28 | 17.8 | - | - | 8.0 | 27.63* | 9.13* |
| DenseNet-161 ($k = 48$) | 28.5 | 22.33* | 6.15* | RKNet-1 \times 3_1 \times 3_1 \times 5_1 \times 2 | 22 | 28.2 | - | - | 12.2 | - | - |

Table 3. Classification errors on ImageNet validation set with a single-crop (224×224). k is growth rate. m_1 , m_2 and m_3 are the number of convolution filters in transition layer 1, 2 and 3 respectively with growth rate k as a unit. For each network model in this table, m_1 is $4k$ as well as m_2 is $8k$ so they are not listed. All the RKNets are the variants of corresponding DenseNets in the same row with similar input dimensions of periods. All the DenseNets in this table have bottleneck and compression rate 0.5 though their names do not contain -BC following [7]. The results with * are run with a batch size of 128 for 100 epochs while the others are trained with a batch size of 256 for 90 epochs.

| Original model | Param (M) | Error (%) | Variant | Error (%) | Param with share (M) | Error with share (%) |
|----------------|-----------|-----------|---|-----------|----------------------|----------------------|
| ResNet-20 | 0.27 | 7.27 | RKNet-1 \times 3_1 \times 2_1 \times 2 | 7.60 | 0.17 | 8.32 |
| | | | RKNet-3 \times 1_2 \times 1_2 \times 1 | 7.57 | - | - |
| ResNet-32 | 0.46 | 6.65 | RKNet-1 \times 5_1 \times 4_1 \times 4 | 7.47 | 0.17 | 8.54 |
| | | | RKNet-5 \times 1_4 \times 1_4 \times 1 | 7.37 | - | - |
| | | | RKNet-1 \times 5_2 \times 2_2 \times 2 | 7.69 | - | - |
| ResNet-44 | 0.66 | 5.82 | RKNet-1 \times 7_1 \times 6_1 \times 6 | 7.69 | 0.17 | 8.84 |
| | | | RKNet-7 \times 1_6 \times 1_6 \times 1 | 7.06 | - | - |
| | | | RKNet-1 \times 7_3 \times 2_3 \times 2 | 7.48 | - | - |
| | | | RKNet-1 \times 7_2 \times 3_2 \times 3 | 7.53 | - | - |
| ResNet-56 | 0.85 | 5.34 | RKNet-1 \times 9_1 \times 8_1 \times 8 | 6.87 | 0.17 | 7.73 |
| | | | RKNet-9 \times 1_8 \times 1_8 \times 1 | 6.72 | - | - |
| | | | RKNet-3 \times 3_4 \times 2_4 \times 2 | 7.05 | - | - |
| | | | RKNet-1 \times 9_2 \times 4_2 \times 4 | 7.08 | - | - |
| ResNet-110 | 1.7 | 5.34 | RKNet-1 \times 18_1 \times 17_1 \times 17 | - | 0.17 | 8.66 |

Table 4. Test errors evaluated on CIFAR-10 with data augmentation. There is no bottleneck used in them. The results of original ResNets are obtained under the experimental settings in this paper. All the RKNets in this table are variants of each other with the same input dimension and different stages or time-steps in every period. In addition, the one-stage variants not sharing weights and biases have the same number of parameters with the ResNets in the same row since only the places of some ReLUs are different between them.

the transformation rules described in 3.1 are evaluated.

The network models reported by [7] are used as experimental objects for comparison. The compression factor is 0.5 for DenseNet-BC which is the same value in [7]. The test error rates on CIFAR-10 are shown in Table 1.

According to the experimental data on CIFAR-10, every one-stage variant has the least parameters among the variants with the same input dimensions and the same number of convolution layers in each period. Sharing weights and biases of convolutions across time-steps in every period decreases the parameters of the one-stage variants further. Especially for DenseNet-BC, the number of parameters is reduced to less than a half of the original value. Nevertheless, the transformation approach described in 3.1 does not

enhance the parameter efficiency of DenseNets without bottleneck and compression effectively. Since DenseNet-BC is more parameter efficient than DenseNet without bottleneck and compression originally, the emphasis of feasibility verification is focused on DenseNet-BC. As a result, only the variants for DenseNet-BC are evaluated on CIFAR-100 and ImageNet. The test error rates on CIFAR-100 are shown in Table 2. The top-1 and top-5 error rates on ImageNet validation set with a single-crop (224×224) are shown in Table 3.

For all the three datasets, similar accuracies are obtained by the variants comparing to the original DenseNets but the performance of one-stage variants on CIFAR-100 and ImageNet is not as good as on CIFAR-10. In addi-

tion, the one-stage variants not sharing weights and biases have higher accuracies than the corresponding variants with shared weights and biases. From the experimental data on CIFAR-10, some variants gain higher accuracies with fewer parameters than DenseNets no matter whether these variants share weights and biases or not.

4.2. Variants of ResNets

Since the building blocks of ResNet resemble the one-stage Runge-Kutta method taking several time-steps except the ReLU at the end of each block, some ResNets are transformed to the variants with different stages or time-steps following the rules in 3.2.

The network models reported by [5] are employed as experimental objects for comparison. The test error rates on CIFAR-10 are shown in Table 4.

From the experimental data, the variants of ResNets are not able to obtain the comparable accuracies with the same number of parameters as ResNets. Moreover, the variants with shared weights and biases do not gain acceptable accuracies either. Hence, the transformation approach for ResNet in 3.2 is not able to obtain the efficient RKNets.

5. Conclusion

A series of numerical analysis methods, Runge-Kutta methods, are employed to construct CNN for image classification task. This kind of CNN is named RKNets in this paper. In order to study the feasibility to apply Runge-Kutta methods, DenseNets and ResNets are varied to RKNets for comparison. The experimental results of DenseNets demonstrate that some RKNets are superior to DenseNets with fewer parameters and higher accuracies. Thus, RKNets can be treated as a basic network architecture to create new network models for image classification and other similar visual tasks as well as even non-visual tasks. However, the experimental results of ResNets indicate that an efficient RKNets is not easy to be achieved although a network model can be constructed lightly basing on the framework of RKNets. Hence, many aspects need further investigation for RKNets to improve its effectiveness. The stage of Runge-Kutta methods and the number of time-steps are obviously two factors affecting the performance of a RKNets. Not only that, but the dimension of each period, the convolutional subnet emulating the increments or changing rates, the coefficients of Runge-Kutta methods, the structure of the pre-processor, transition layers and postprocessor, the effects of time as well as the connections between the non-adjacent periods are also the important influence factors to perfect RKNets.

On the other hand, RKNets could help to make it clear what was the meaning of each component in a network model and what was its relationship with the visual cortex. Then, the inspiration could be drawn from neuroscience to

improve the artificial neural network. At the same time, mathematical approaches could be applied more widely on constructing neural network models and even the description of visual system finally.

References

- [1] Peter Dayan and Laurence F Abbott. *Theoretical neuroscience*, volume 806. Cambridge, MA: MIT Press, 2001.
- [2] Melvyn A Goodale and A David Milner. Separate visual pathways for perception and action. *Trends in neurosciences*, 15(1):20–25, 1992.
- [3] Sam Gross and Michael Wilber. Training and investigating residual nets. February 2016.
- [4] Kaiming He, Xiangyu Zhang, Shaoqing Ren, and Jian Sun. Delving deep into rectifiers: Surpassing human-level performance on imagenet classification. In *The IEEE International Conference on Computer Vision (ICCV)*, December 2015.
- [5] Kaiming He, Xiangyu Zhang, Shaoqing Ren, and Jian Sun. Deep residual learning for image recognition. In *The IEEE Conference on Computer Vision and Pattern Recognition (CVPR)*, June 2016.
- [6] Andrew G Howard. Some improvements on deep convolutional neural network based image classification. In *International Conference on Learning Representations*, 2014.
- [7] Gao Huang, Zhuang Liu, Laurens van der Maaten, and Kilian Q. Weinberger. Densely connected convolutional networks. In *The IEEE Conference on Computer Vision and Pattern Recognition (CVPR)*, July 2017.
- [8] Alex Krizhevsky. Learning multiple layers of features from tiny images. 2009.
- [9] Alex Krizhevsky, Ilya Sutskever, and Geoffrey E Hinton. Imagenet classification with deep convolutional neural networks. In *Advances in neural information processing systems*, pages 1097–1105, 2012.
- [10] Ming Liang and Xiaolin Hu. Recurrent convolutional neural network for object recognition. In *The IEEE Conference on Computer Vision and Pattern Recognition (CVPR)*, June 2015.
- [11] Q. Liao and T. Poggio. Bridging the Gaps Between Residual Learning, Recurrent Neural Networks and Visual Cortex. *ArXiv e-prints*, April 2016.
- [12] Tsung-Yi Lin, Michael Maire, Serge Belongie, James Hays, Pietro Perona, Deva Ramanan, Piotr Dollár, and C Lawrence Zitnick. Microsoft coco: Common objects in context. In *European conference on computer vision*, pages 740–755. Springer, 2014.
- [13] Geoff Pleiss, Danlu Chen, Gao Huang, Tongcheng Li, Laurens van der Maaten, and Kilian Q Weinberger. Memory-efficient implementation of densenets. *arXiv preprint arXiv:1707.06990*, 2017.
- [14] Olga Russakovsky, Jia Deng, Hao Su, Jonathan Krause, Sanjeev Satheesh, Sean Ma, Zhiheng Huang, Andrej Karpathy, Aditya Khosla, Michael Bernstein, et al. Imagenet large

scale visual recognition challenge. *International Journal of Computer Vision*, 115(3):211–252, 2015.

- [15] Karen Simonyan and Andrew Zisserman. Very deep convolutional networks for large-scale image recognition. In *International Conference on Learning Representations*, 2015.
- [16] Christian Szegedy, Wei Liu, Yangqing Jia, Pierre Sermanet, Scott Reed, Dragomir Anguelov, Dumitru Erhan, Vincent Vanhoucke, and Andrew Rabinovich. Going deeper with convolutions. In *The IEEE Conference on Computer Vision and Pattern Recognition (CVPR)*, June 2015.
- [17] Yi-Jen Wang and Chin-Teng Lin. Runge-kutta neural network for identification of dynamical systems in high accuracy. *IEEE Transactions on Neural Networks*, 9(2):294–307, 1998.